J. Phys. Earth, **24**, 63-87, 1976

A SEARCH INTO THE FAULTING MECHANISM OF THE 1891 GREAT NOBI EARTHQUAKE

Takeshi MIKUMO and Masataka ANDO*

Disaster Prevention Research Institute, Kyoto University, Uji, Kyoto, Japan

(Received July 28, 1975; Revised October 20, 1975)

The 1891 Nobi earthquake was the greatest ($M \cong 8$) inland earthquake in Japan, which was accompanied by surface fault breaks extending over 80 km, with unusually large displacements with a maximum displacement of 8 m, and also caused pronounced vertical and horizontal tectonic movements, extremely strong ground motions and heavy seismic damage. All these geophysical and geological data are used together to recover the general features of the faulting mechanism from a modern seismological viewpoint based on dislocation theories.

The fault rupture seems to have initiated at a depth around the northwestern end of the fault, and propagated southeastwards almost unilaterally at velocities of about 2.5 km/sec, forming successive fault slips with a sliding velocity of probably over 100 cm/sec, down to at least 15 km depth along three major preexisting Quaternary faults. The rupture propagation was temporarily blocked probably by the curvature of the fault traces or by small lateral heterogeneities at the southern end of the Neodani fault, and then branched off into two directions iucluding along a deep latent fault extending southward. All seismic faulting appears to have been completed within 40 sec.

A uniform geology in basement rocks covering a wide region is considered to have allowed the formation of this long fault. The released stresses are estimated to be 40-150 bars, which appear appreciably different from one place to another. Unusually large displacements and stresses in the southern part of the Neodani fault may be attributed to the nature of the fault plane there. A part of the stresses appears to have been released by a small amount of aseismic slip that continued for longer than 20 years. Possible sources of the stresses that caused this great earthquake are also discussed.

1. *Introduction*

The Nobi (Mino-Owari) earthquake of October 28, 1891, which occurred in central Honshu, was the greatest inland earthquake ever experienced in

* Now at National Center for Earthquake Research, U.S. Geological Survey, Menlo Park, California 94025, U.S.A.

Japan. Its magnitude has been estimated as 7.9 according to the present JMA scale (JMA, 1957), and also re-estimated as about 8.0 by MURAMATU (1962) from the distribution of seismic intensities. This earthquake was very unique among a number of large earthquakes in Japan in that it resulted in remarkable surface fault breaks which could be clearly traced as long as 80 km with maximum horizontal and vertical displacements of 8 m and 3 m respectively, and also caused heavy seismic damage over an extensive area. The reported damage in and around the epicentral area was: 7,273 people dead and 17,175 injured, 142,177 houses collapsed and 80,184 damaged, and over 10,000 landslides (USAMI, 1966). A number of seismological and geological studies were made after the earthquake, and various results have been reported to date. The fault breaks that emerged on the ground surface gave a clue to assess the cause of this great earthquake, and the notion that faulting motion was the source of the earthquake and not its result was presented by KOTO (1893) immediately after the earthquake. This idea has been undoubtedly demonstrated to be correct by theory more than 70 years later.

We attempt to investigate here the faulting mechanism of this greatest inland earthquake, from a modern seismological point of view based on dislocation theory, combining all available geophysical and geological data. The main purpose of the present study is to clarify the dynamical processes of the initiation and formation of faulting, and also to consider possible causes of the faulting with its unusually large displacements over a long distance. Another purpose is to predict seismic ground motions that would be expected to arise from future destructive earthquakes of comparable magnitudes and with a similar mechanism to that of the Nobi earthquake. This would provide a basis for observational projects for future large earthquakes as well as for earthquake engineering purpose.

2. *Data*

There is some difficulty in discussing the detailed mechanism, due to the lack of reliable seismic observations at the time of the 1891 Nobi earthquake. However, there are geological and geophysical data now available which include the following:

1) Location and orientation of surface fault breaks and fault displacements,
2) Distribution of aftershocks and related microseismicity around the fault area,
3) Distribution of seismic intensities,
4) Vertical and horizontal tectonic ground movements,
5) Predominant directions of ground motion at various sites,

6) Old seismograph records at two nearby stations.

These data are used together here to infer the general features of the faulting processes. The first four sets of data can be used to estimate the dimensions and orientation of the fault plane and average fault displacement over the plane, stress drop etc., and the last two sets of data together with 3) provide information on dynamical parameters such as the initial point of fault rupture, sliding velocity of the fault surfaces and velocity of rupture propagation.

2.1 Surface fault breaks

A long train of surface fault breaks that appeared during this earthquake has been elaborately traced by KOTO (1893) and OMORI (1910) and reconfirmed by BESSHO (1967), and it was found that it extended along Nojiri (a)–Nukumi (a')–Midori–Kinbara–Takatomi–Katabira (d), as illustrated in Fig. 1. The detailed field surveys recently made by MATSUDA (1974) have revealed the

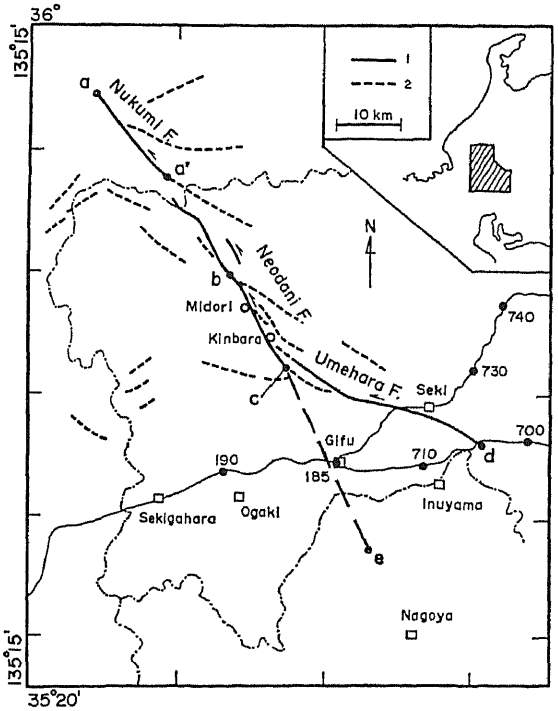

Fig. 1. Location of the fault traces in the Nobi earthquake area (modified from MATSUDA's paper, 1974). 1. surface fault breaks made during the 1891 Nobi earthquake, 2. pre-existing active Quaternary faults. Fine curves with numbered circles show the leveling routes with the locations of bench marks.

overall features of the surface faulting extending for about 80 km in a general direction of N45°W. His comprehensive results have greatly encouraged us to make further studies into the faulting mechanism of this earthquake.

Figure 1, which is a somewhat modified figure from MATSUDA's paper (1974), shows that a number of pre-existing Quaternary faults in this region trend mainly in the NW-SE direction and in some cases in the NE-SW direction, and that they form a conjugate set of strike-slip faults termed as the Nobi fault system. MATSUDA (1974) pointed out that the surface faulting from the earthquake resulted mainly from left-lateral displacements of three major pre-existing faults, i.e. the Nukumi, Neodani and Umehara faults, but that the surface breaks did not appear over the entire length of each fault. The fault length and displacements revealed by MATSUDA's surveys (1974) are again summarized in Table 1. The orientations of the surface faults are found

Table 1. Surface fault displacements (after MATSUDA, 1974).

(1)	Nukumi fault: Nojiri(a)–Nukumi(a'), 20 km, strike N40°W horizontal displacements; left-lateral, maximum 3 m, average about 1 m vertical displacements; SW-side up, maximum 1.8 m, average about 1 m
(2)	Neodani fault: Mt. Hakusan–Nogo–Midori–Kawauchi(c), 35 km, strike N40°W horizontal displacements; left-lateral, maximum 8 m, average 3 m (north), 7 m (south) vertical displacements; SW-side up, maximum 4 m, average 3 m (north), 0 m (south)
(3)	Umehara fault: Kawauchi(c)–Seki–Sakakura(d), 25 km, strike N60°W horizontal displacements; left-lateral, maximum 5 m, average about 1.5 m vertical displacements; SW-side up, maximum 2.4 m, average about 2 m

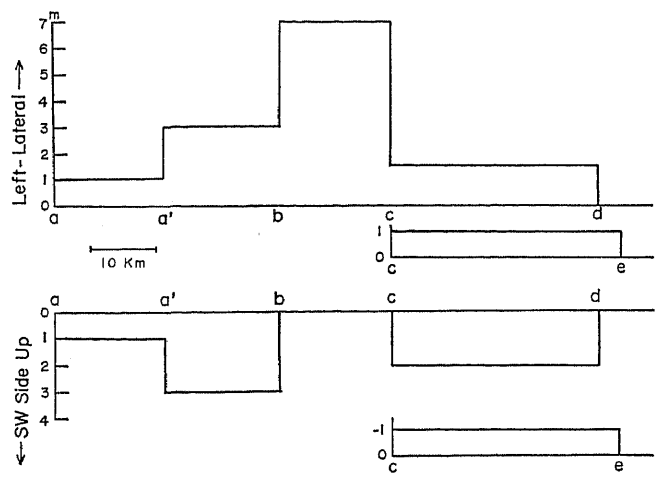

Fig. 2. Average horizontal and vertical displacements for each segment of the faults, which are smoothed from MATSUDA's results (1974). Letters a, a', b, c, d and e correspond to the positions given in Fig. 1. Displacements for a latent fault c–e are the assumed values.

to be almost vertical except for a few localities. The average displacements of the three faults are illustrated in Fig. 2, which have been smoothed from MATSUDA's results (1974). Also note that there are a few minor fault breaks with lengths shorter than 1 km; these are the Kurotsu, Midori-Daishogun, Midori and Koze (MATSUDA, 1974). Among them, the Midori fault in the Neodani village has been made famous by KOTO's photograph (1893). It is a spectacular fault scarp that extends over 400 m with a vertical displacement of 6 m (NE-side up) and a left-lateral horizontal displacement of 4 m. However, this fault movement was an exceptional feature among the overall down movement of the NE-side throughout the Neodani fault, and hence has been an object of long debates. MATSUDA (1974) has given an interpretation that this was caused by a local bulge of the Midori triangular area due to compressive forces resulting from curved strike-slip movements. In this paper, these local movements will be omitted, to a first approximation, although they are still of some importance.

2.2 Aftershocks

It was reported by the GIFU OBSERVATORY (1894) that 3,090 aftershocks had been felt there for 14 months after the Nobi earthquake. The aftershock activity has continued for many years, with a decaying rate of $n(t) \propto t^{-1.05}$ (UTSU, 1969), and 3–4 shocks per year are still observed even in recent years. Seismic observations of micro- and ultramicro-earthquakes were recently made near the fault zone by several university groups (MURAMATU *et al.*, 1963; MIKI *et al.*, 1965; WATANABE and NAKAMURA, 1967; OOIDA *et al.*, 1971). The results indicate that the microearthquake activity is still high in the area just southwest of the Neodani fault and also between Gifu and Inuyama (See Fig. 1). These areas of high seismicity may be zones of aftershock activity in view of their locations. The focal depths are mainly confined to be shallower than 15 km, which would suggest either that the lower limit of the fault plane extends down to that depth, or that physical properties of rock materials there do not allow minor brittle fractures below this depth.

2.3 Seismic intensity distribution

OMORI has investigated (1894) ground accelerations during the Nobi earthquake from the extensive distribution of squared bodies such as stone monuments, tomb stones, etc. that fell down or collapsed by strong ground shaking. The maximum accelerations exceeded 400 gals (OMORI, 1894). The zone of large accelerations ran along a fault line extending from Nukumi–Neodani–Takatomi, which had been revealed by his own field surveys, and also branched off south of Neodani extending southwards through Gifu–Ichinomiya to near Nagoya. MURAMATU (1963) also estimated the distribution

of seismic intensities from the areal distribution of completely collapsed houses and various surficial ground deformations. Taking into account the existence of a boundary line between tectonic uplift and subsidence, he concluded that a deep latent fault might branch off around Kinbara and reach north of Nagoya. This conclusion seems to be supported indirectly by a relation between the collapsed rates of houses and the thickness of alluvial layers (YOKOO and HORIUCHI, 1969), geological inferences on the possible existence of Ichinomiya–Inazawa fault (SUGISAKI and SHIBATA, 1961), and also by some discontinuity of gravity anomalies across this line (IIDA and AOKI, 1959).

3. *Fault Model*

From the various evidence described in the foregoing sections, we consider that the three major faults probably form nearly vertical fault planes linked together below some depth. The lower limit of the fault plane lies, at least, at a depth of 15 km, in view of the aftershock activity. Since the depth is not accurately known, we assume several probable values such as 10, 15, 20 and 25 km in later discussions. The dislocations over the fault plane may be governed by stress distribution prior to the earthquake, and cannot be constant but would decrease with depth. Since it is difficult to estimate directly such a decreasing trend, we assume constant dislocations with depth for each segment of the faults, taken from the surveyed surface fault displacements (MATSUDA, 1974). We also consider the possible existence of a latent fault c–e, as in Fig. 1, although any clear surface breaks cannot be traced along this line except small-scale ground fissures (MURAMATU, 1963). The southern end (e) cannot be fixed, but the length of c–e is tentatively assumed as 34 km, which reaches south of Ichinomiya. There is no direct evidence for displacements of this latent fault. We assume various values ranging from 1 to 3 m for the NE-side up and left-lateral motion. The sense of the vertical motion is opposite to that of the other faults, but is consistent with the west-side down movement of the presumed Ichinomiya–Inazawa fault (SUGISAKI and SHIBATA, 1961). In Fig. 2, the case of 1 m displacements is shown.

The case for fault movements of the three major faults a–a′, a′–b–c and c–d is hereafter called Case A, and the case including the latent fault (c–e) movement is named Case B. Which of the two cases better explains the observations will be tested in the light of tectonic movements and direction of ground motion in later sections.

4. *Coseismic Tectonic Movements*

Leveling surveys around the fault zone were made in 1885–1888 prior to

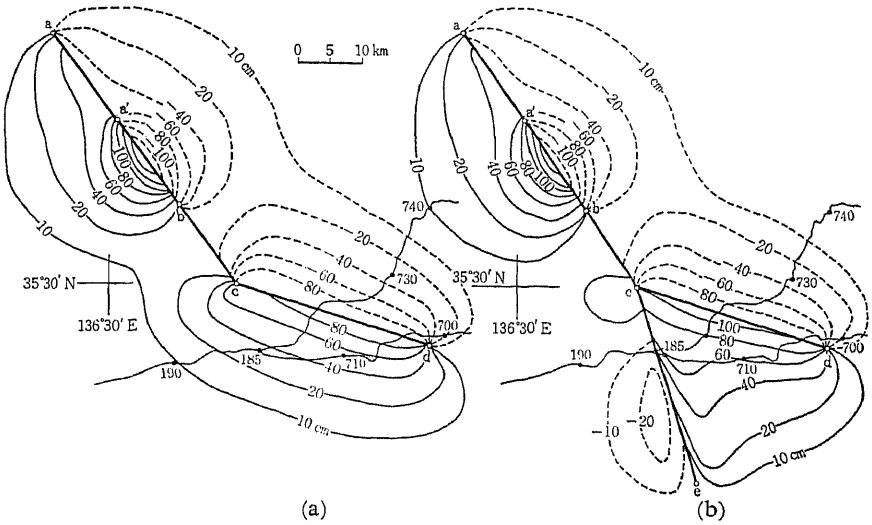

Fig. 3. Pattern of the computed vertical displacements from two different fault models. (a) Case A without a latent fault c-e, (b) Case B with the latent fault. Solid and broken curves show contour lines of uplift and subsidence, respectively.

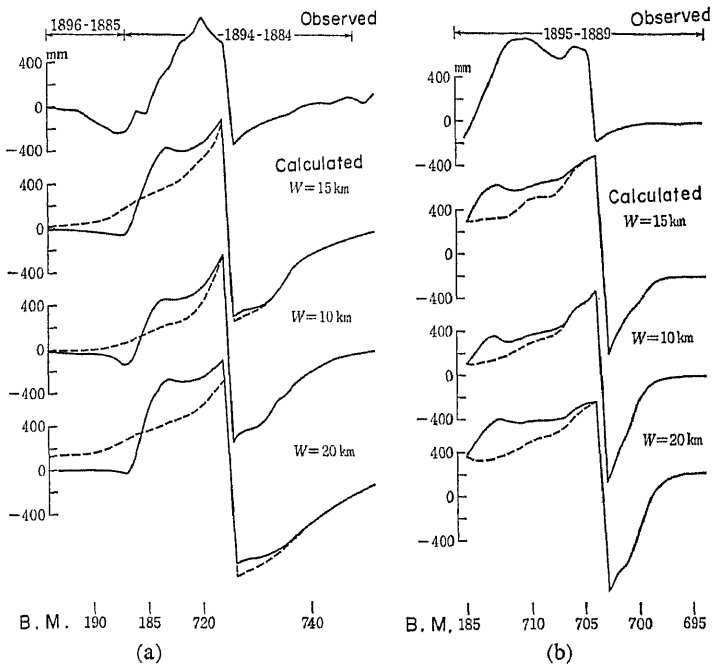

Fig. 4. Observed and computed vertical displacements along two leveling routes. (a) B.M. 190–740, (b) B.M. 185–695. Observed displacements refer to the results of the GEOGRAPHICAL SURVEY INST. (1973). Solid and broken curves for the computed displacements correspond to Case B and Case A, and W indicates the fault depth.

the Nobi earthquake and again in 1894–1898 after the earthquake by the Military Land Survey (presently the Geographical Survey Institute of Japan) (MUTO and KAWABATA, 1933). Two leveling routes across the southern part of the fault traces (B.M. 190–185–740 and 185–700) are shown in Figs. 1 and 3. A noticeable feature is the pronounced crustal uplift of about 70 cm near B.M. 720 (between Gifu and Seki) and also appreciable subsidence of 30–40 cm east of Seki (J. 725) and west of Ogaki (B.M. 189) (GEOGRAPHICAL SURVEY INST., 1973), which can be seen from the uppermost trace of Fig. 4(a). MURAMATU (1963) has compiled a contour map of the ground uplift and subsidence on the basis of the leveling surveys, surface fault traces and distribution of earthquake damages.

On the other hand, triangulation surveys were also made in the southern part of the fault area before and after the earthquake by the Land Survey (SATO, 1974). Horizontal tectonic movements associated with the earthquake have been estimated from the pre- and post-seismic surveys, and have recently been re-calculated by SATO (1974) only from 1st and 2nd order triangulation results, assuming that three stations, Gozaishoyama, Nabeyama and Mikawahongu were fixed. His results are reproduced in Fig. 5, which shows horizontal displacements of the order of 1 m directed generally towards the southeast.

We calculate here theoretical vertical and horizontal displacements from the above fault models and compare them with the above measurements. The method of calculation is based on the formulations given by MARUYAMA (1964) and also by MANSINHA and SMYLIE (1971) for static dislocations in a half space. Figures 3(a) and (b) show the pattern of the vertical displacements computed for Cases A and B, respectively. For Case B, the upper rim of the fault c–e is assumed to reach 2 km below the ground surface, and its horizontal and vertical fault displacements are taken to be 1 m. It is immediately noticed that an area of subsidence emerges west of c–e in Case B, and that this pattern is similar to that of the contour map compiled by MURAMATU (1963). A closer examination reveals, however, that the decay of the measured displacements away from the fault traces appears more rapid than the computed patterns.

In Figs. 4(a) and (b) are compared the measured and computed vertical displacements along the two leveling routes. Computations have been made for fault depths of 15, 10 and 20 km, and solid and broken curves correspond to the cases with and without the latent fault (Cases B and A) respectively. It is evident that Case A would not be able to account for the measurements particularly for a marked subsidence around B.M. 180–190. Case B, on the other hand, yields slightly smaller subsidence just west of c–e and larger subsidence just east of the Umehara fault, as compared with the measurements.

These discrepancies, however, may be reduced by adjusting the vertical component of displacements over the two faults. We also notice that the depth of the fault plane has little effect on the general pattern and the absolute displacements. This suggests that it would be rather difficult to estimate the fault depth to a precision of 5 km.

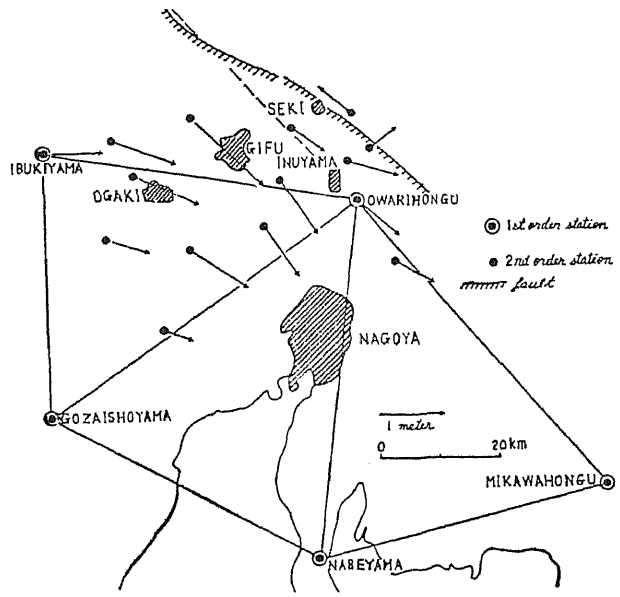

Fig. 5. Horizontal displacements re-calculated by SATO (1974) from triangulation data. In this calculation, three points, Gozaisho-yama, Nabeyama and Mikawa-Hongu are fixed.

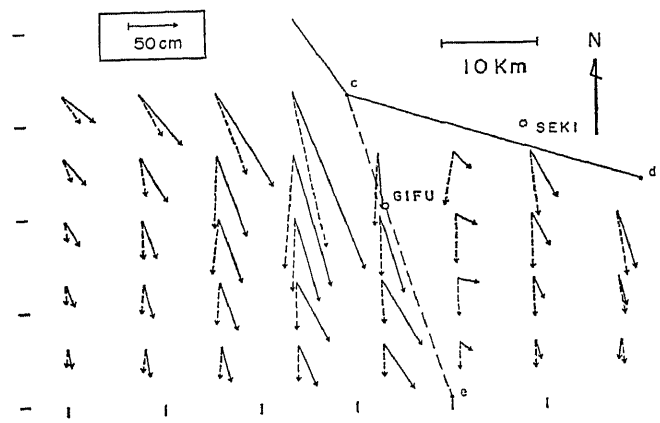

Fig. 6. Computed horizontal displacements from two fault models. Solid and broken arrows indicate Case B and Case A respectively, and fine solid line c–d and broken line c–e are the fault traces.

The horizontal displacements computed for several sites near the southern fault zone are illustrated in Fig. 6, where solid and broken arrows indicate those for Cases B and A. If we compare these patterns with the observations shown in Fig. 5 (SATO, 1974), the directions from Case B appear to give a better agreement, whereas Case A generally yields southward displacements. The directions just east of the fault trace c–e are rather sensitive to its fault displacement. In this figure, we take 1.5 m for its vertical and horizontal components. Smaller displacements make these directions more southward and larger displacement direct them more northeastward.

The above comparison between the measurements and computed results clearly indicates that most of the large tectonic movements were of coseismic displacements, and that faulting motion took place also along the latent fault c–e. It also appears that average fault displacements of the Umehara fault may be considerably smaller than those expected from the surface fault offsets, suggesting decreasing dislocation with depth, and that displacements of the fault c–e may be unexpectedly large.

A NE-side upthrown movement of the latent fault and a SW-side up movement of the Umehara fault elevated a triangular area c–d–e bounded by the two faults, and hence may have caused a concentration of local stress in the area. The fact that microearthquakes are still taking place in the area (WATANABE and NAKAMURA, 1967; OOIDA *et al.*, 1971) may be explained as aftershock activity by the re-adjustment of the concentrated stress.

5. *Direction of Ground Motion and Old Seismograph Records*

5.1 *Direction of ground motion*

During the Nobi earthquake, a great many houses collapsed in the "meizoseismal area," but the directions of collapse were not systematic (OMORI, 1894). This direction probably depends on the shape and structure of the houses and does not always represent the direction of ground motion. OMORI (1894, 1900) used, instead, falling directions of a number of cylindrical bodies such as stone lanterns, tomb stones, chimneys etc., to estimate predominant directions of ground motion at various sites. The directions were somewhat irregular at some places, but very uniform at other places (OMORI, 1894). As an example of the latter case, an average direction at Nagoya was estimated to be N60°E→S60°W from 200 observations (OMORI, 1894, 1900), and its standard deviation calculated from his data is 26°. His data show that the directions thus estimated at Ogaki, Kitakata, Inuyama, Tsushima, Nagoya and Kuwana in the southern part of the fault area seem most reliable and those at Gifu and Ichinomiya follow the above. These directions are shown

by the solid arrows in Fig. 11, which appear nearly perpendicular to the axis of "meizoseismal zone" (OMORI, 1894).

5.2 Old seismograph records

The Nobi earthquake was recorded by old strong-motion seismographs at Gifu, Nagoya, Osaka and Tokyo (GIFU OBSERVATORY, 1894), but only the records from the first two stations are now available. Unfortunately, however, only the initial portion of ground motion was recorded with up to about 7 sec after triggering of the recorder at Gifu and 13–15 sec at Nagoya, as can be seen in the uppermost traces of Figs. 12 and 13, and after that time the records went off scale probably due to the arrival of large amplitude S waves. The magnification of the horizontal and vertical seismographs was about 5–5.5 and 8–9, respectively (GIFU OBSERVATORY, 1894). The natural period and damping constant are not known, but may be guessed as about 3 sec and 0.1 (no damper but with pen-tip friction), if the seismographs were of the Milne type which had been conventionally employed at that time. Since these two stations were very close to the fault zone, the records are still very useful in providing information on the faulting process. Besides these records, simple seismoscopes had recorded only the trace of initial ground motions at Gifu and other two sites (GIFU OBSERVATORY, 1894). It seems that there were no seismometric observations of the earthquake outside Japan, as far as we know.

6. Inferences on Faulting Process

In this section, we attempt to infer the overall faulting processes. To do this, we calculate theoretically dynamic ground displacements that would be expected for various cases, and compare the resultant directions of ground motions and synthetic seismograms with the corresponding observations. For this calculation, we refer to the dynamic dislocation model in an infinite elastic medium given by MARUYAMA (1963) and HASKELL (1969), with a simple correction for the free surface. Horizontal ground motion can be obtained by a vectorial combination of two components (ABE, 1974), and synthetic seismograms are computed by taking a convolution of the ground displacements with the impulse response of the seismograph (MIKUMO, 1973a).

For static parameters including fault orientations, dimensions and average displacements, we use the already estimated values in the foregoing sections. Dynamic ground displacements depend also on the starting point, propagation velocity and direction of fault rupture, and rise time of fault displacements. We consider three different cases for the starting point of fault rupture; a, the northern end of the Nukumi fault; b, the middle point of the Neodani fault;

and c, the branch point to the Umehara fault and to the latent fault. In all cases the rupture is assumed to be initiated at the half depth of the fault plane and to propagate radially at a constant velocity over the plane. Since the entire fault length is long as compared to the fault depth, case a is similar to unilateral faulting and cases b and c to bilateral. Computations have been made for rupture velocities of 2.2, 2.5 and 3.0 km/sec, and also for three different combinations of rise times, 1) 2.0 sec throughout the entire fault, 2) 1.0, 2.0, 3.5, 1.5 and 1.0 sec for fault segments a–a′, a′–b, b–c, c–d and c–e, respectively, depending on the fault displacements (the sliding velocity of the fault plane is about 100 cm/sec throughout the entire fault), and 3) 1.5, 4.0, 7.0, 2.5 and 1.5 sec for each of the segments (sliding velocity is about 50 cm/sec throughout). The crustal P and S wave velocities are taken to be 6.0 and 3.5 km/sec from the results of seismic explosion observations around this region (SASAKI *et al.*, 1970; AOKI *et al.*, 1972).

Figure 7 shows the horizontal ground motion diagrams in several different cases computed for Gifu which is situated very close to the fault zone. Letters a, b and c indicate the starting point of fault rupture, and τ and v are the assumed rise time and rupture velocity (2.5 km/sec if not specified). The solid and broken curves correspond to Cases A and B, and the numerals indicated

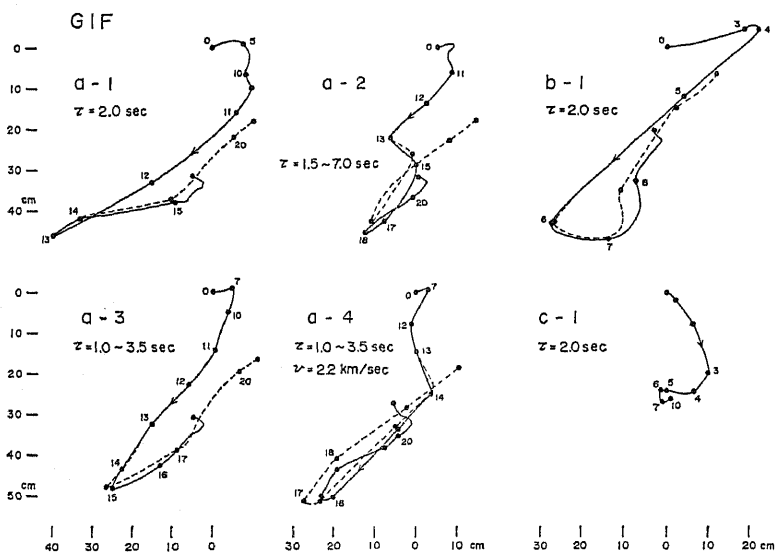

Fig. 7. Horizontal ground motion diagrams at Gifu computed for various faulting processes. a, b and c indicate the assumed initial point of fault rupture, which correspond to the positions in Fig. 1. τ; rise time of fault displacement, v; rupture velocity, 2.5 km/sec if not specified. Solid and broken curves correspond to Cases A and B. Numerals on each curve indicate the elapsed time after the arrival of P wave first motions.

on the curves are the time (in sec) elapsed after P wave arrival. We see that the patterns of the ground motion are generally similar except for c–1, but change slightly with different rise times and rupture velocities.

Figures 8, 9 and 10 are similar diagrams for six sites; Ogaki (OGK), Gifu

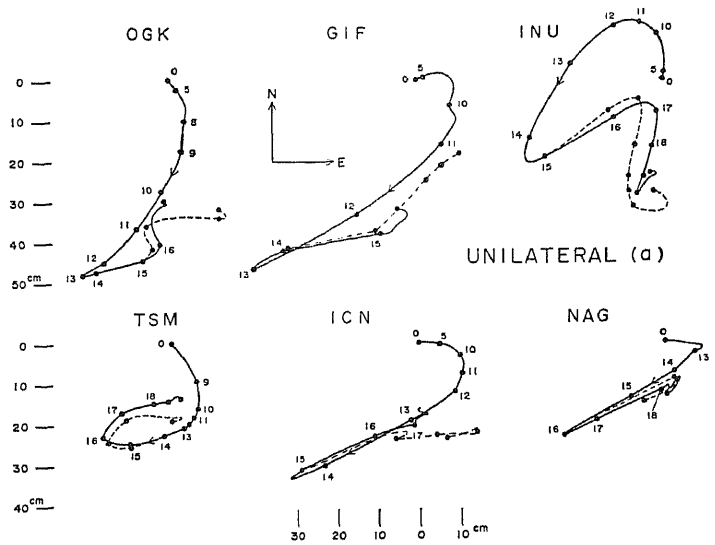

Fig. 8. Computed horizontal ground motions at six sites, in the case of faulting initiated at a, with $\tau=2.0$ sec throughout and $v=2.5$ km/sec.

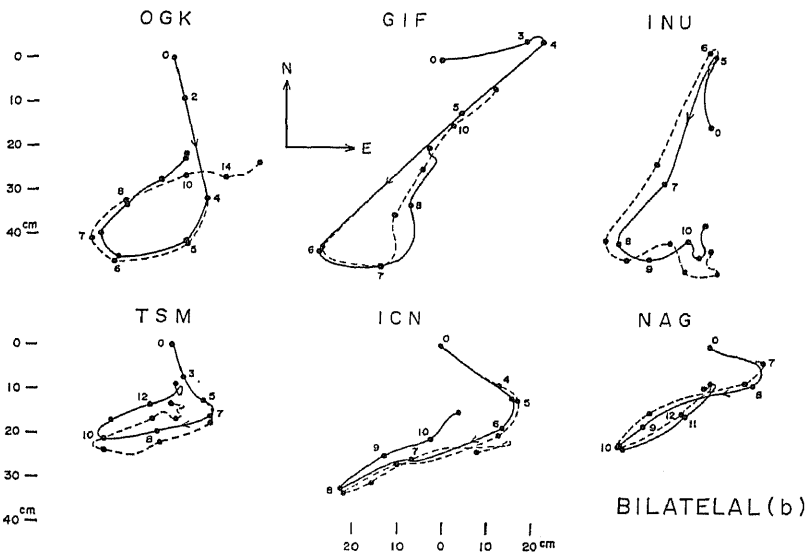

Fig. 9. Computed horizontal ground motions at six sites, in the case of faulting initiated at b. For other explanations, refer to Figs. 7 and 8.

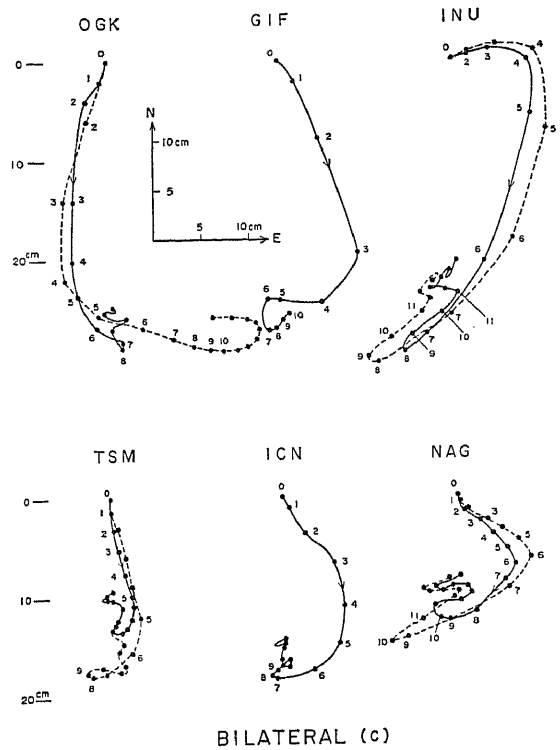

Fig. 10. Computed horizontal ground motions at six sites, in the case of faulting initiated at c. For other explanations, refer to Figs. 7 and 8.

(GIF), Inuyama (INU), Tsushima (TSM), Ichinomiya (ICN) and Nagoya (NAG) for three different cases, a, b and c, respectively, but with the same values of $\tau=2.0$ sec and $v=2.5$ km/sec. We immediately notice that there are significant differences in the absolute amplitudes, the directions of maximum velocity or predominant directions of ground motion at each of the sites, among the three cases. The directions of maximum velocity in case a, which are indicated by an arrow on each of the curves in Fig. 8, are represented in Fig. 11 by the broken arrows. Note that these calculated directions parallel closely the predominant directions of ground motion (solid arrows) estimated by OMORI (1894) except for Ichinomiya. The disagreement for the last site may be due to insufficient data collected by Omori. The directions estimated by him for Inuyama and Kuwana are in almost reverse sense to the calculated directions. This is not important, however, because the overturning of cylindrical bodies will depend on their stability against short-period vibrations, and because the calculated ground motion does not involve periods shorter than several seconds. The general agreement except for the sense appears

to suggest that short-period waves are superposed on longer period ground motion, vibrating in similar directions. It is clear, on the other hand, that the directions calculated for case c do not agree with the directions estimated by Omori. In cese b, the discrepancies are rather small except for Ogaki but are slightly worse than in case a. From this evidence, it may be inferred that a fault rupture was initiated around the northern end of the Nukumi fault (a) or at some point between a and b.

It is interesting to note an account of one witness (MATSUDA, 1974) of the time elapsed after the collapse of houses to the formation of fault displacements near Seki along the Umehara fault. Matsuda's estimate for this time is several sec to a little longer than 10 sec. If the collapse took place due to S waves with maximum ground velocity, we would be able to estimate the elapsed time very roughly, from the time between the initiation of the fault rupture and the arrival of the S waves and the time between the initiation and the formation of fault displacements. A simple calculation yields the elapsed time of 7–10, 3–4 and 2–3 sec for cases a, b and c respectively. The first case seems plausible and is consistent with the inferences described above.

The calculated displacements of the horizontal ground motion reach 60 cm at Gifu and 40 cm at Nagoya in cases a and b, whereas case c yields about one third of the corresponding amplitudes, as can be seen from Figs. 8, 9 and 10. OMORI (1894) has estimated the lower limit of the amplitude at Nagoya to be about 23 cm, using the maximum acceleration necessary for overturning of square bodies and the predominant period (1.3 sec) of P waves recorded on a seismograph. The displacement at Gifu estimated in this way, and the ground velocity at the two stations obtained directly from these estimates, are compared with the calculated values in Table 2. The differences between them may naturally be accounted for mainly by the difference in the wave period involved, and partly by the assumed larger fault displacements, and may not be large enough to effect the appropriateness of the present approximate model. More realistic models including stick-slip faulting, which radiate short period waves, would reconcile the above discrepancies.

In Figs. 12 and 13 two horizontal component seismograms recorded at

Table 2. Maximum ground displacements and velocities.

	Displacements (cm)		Velocities (cm/sec)	
	(1) Estimated	(2) Calculated	(1) Estimated	(2) Calculated
Nagoya	23*	40	54	15
Gifu	34**	60	72	30

* After OMORI (1894), predominant period 1.3 sec.

** Predominant period about 2.5 sec.

Gifu and Nagoya are compared with some examples of the corresponding initial portion of the synthetic seismograms computed for various faulting processes. In these Figs., the initial times of the recorded seismogams have been slightly adjusted, assuming that the onset time triggered by the arrival of first motion P waves might have been delayed by about 1 sec. Letters a, b, v and τ have the same meanings as given in Figs. 7–10. Although the comparison is not complete due to some ambiguities involved and can be made only for a limited time interval, it appears to show that among the computed traces shown here, case a-3 may give fairly good approximations to the actual recorded amplitudes, wave forms and time correspondences of the peaks and troughs except for the NS-component for Nagoya. The recorded large amplitude between 5 and 10 sec cannot be explained by any of the computed seismograms. Case a-4 appears to follow case a-3 in the degree of agreement. Case a-2, on the other hand, gives large amplitudes beginning at 7 sec at Gifu and 10 sec at Nagoya. This is inconsistent with the features of the records which went off scale around 10 sec and 15 sec at the two stations. The better agree-

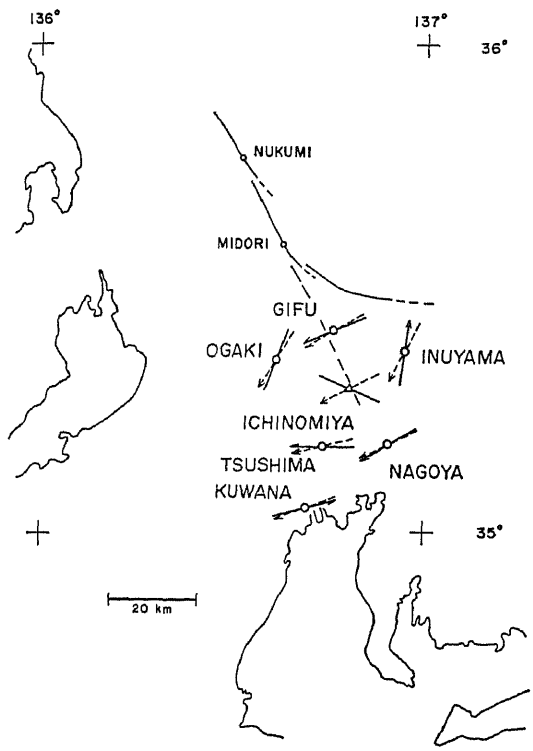

Fig. 11. Predominant directions of ground motion (solid arrows) estimated by OMORI (1894) at several sites, and the computed directions with a maximum ground velocity (broken arrows).

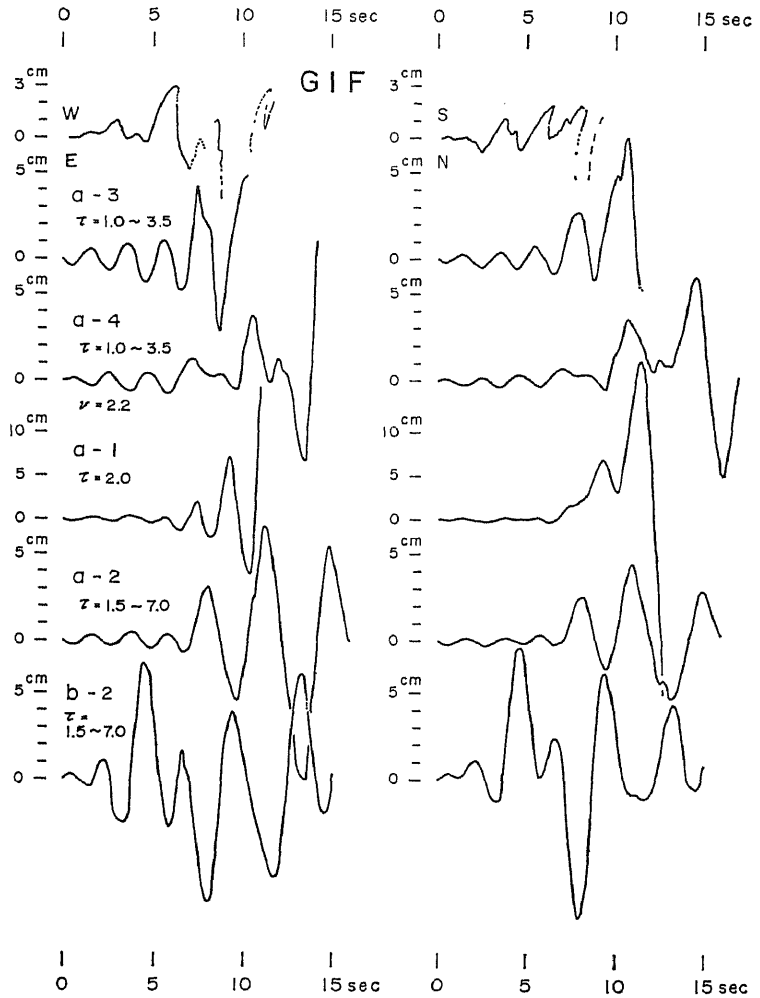

Fig. 12. Two components of the recorded (uppermost traces) and computed synthetic seismograms at Gifu. For letters a, b, τ and v, refer to the explanations in Fig. 7.

ment between the computed traces for case a-3 or a-4 with the records implies that fault displacements at each point may have been completed in a time scale shorter than 4 sec rather than a longer time of 7 sec.

If the fault rupture was initiated at point b, large amplitude S waves would arrive about 3.5 sec after the first P waves at Gifu and about 7 sec at Nagoya, as shown in the lowest traces b-2. Clearly, this is not the case in the recorded seismograms. If the rise times are shorter than those assumed for b-2, the computed amplitudes would be much larger and hence the deviation from the records would become greater. The S-P times read from the

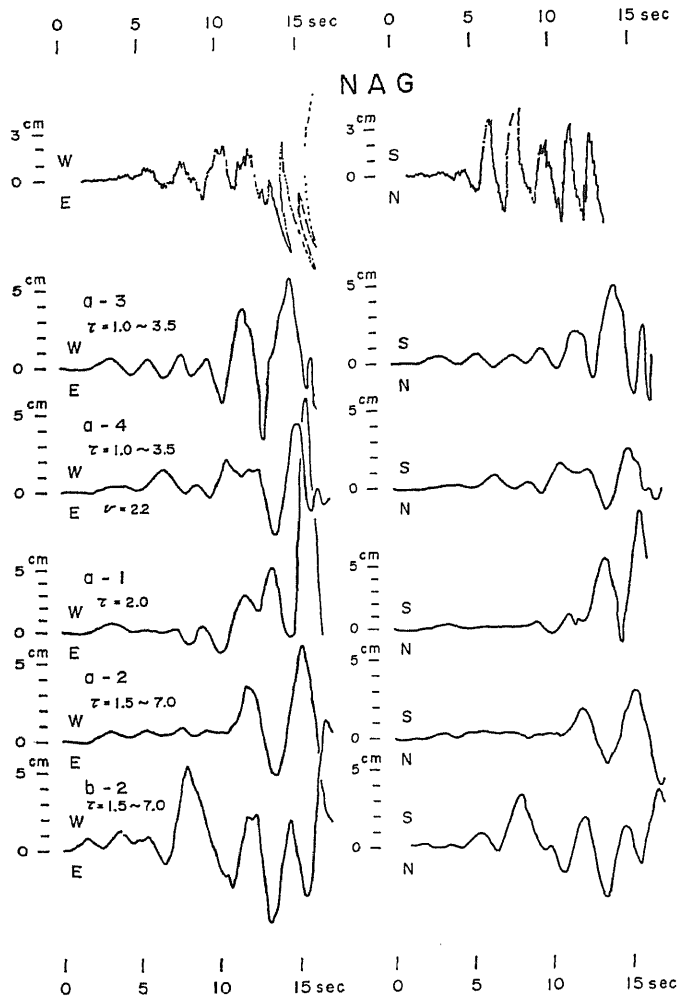

Fig. 13. Two components of the recorded (uppermost traces) and computed synthetic seismograms at Nagoya. For letters a, b, τ and v, refer to Fig. 7.

records are at least 8 sec and 13.5 sec at the two stations, and would locate the starting point of the first seismic waves around point a, using the coefficient $k=v_P v_S/(v_P-v_S)=8.4$ km/sec. This estimate is consistent with that inferred from the direction of ground motion.

7. *Discussion*

7.1 *Formation of faulting*

The location of the epicenter or the Nobi earthquake has long been as-

sumed to lie around Midori-Kinbara (between b and c) along the Neodani fault (e.g. GIFU OBSERVATORY, 1894; KOTO, 1893) on the basis of the largest surface fault displacements and heavy earthquake damages there (MURAMATU, 1963). This interpretation is not completely erroneous, in the sense that the largest faulting motion along this part radiated large amplitude seismic waves, which caused extremely strong ground motions over the Nobi plain and its adjacent regions. However, a synthetic study of the faulting processes based mainly on the directions of ground motion and seismograph records, as well as from tectonic movements, would lead us to the following conclusions: The fault rupture seems to have been initiated at a depth around point a near the northwestern end of the Nukumi fault, and propagated southeastwards almost unilaterally along pre-existing active faults with a rupture velocity of about 2.2–2.5 km/sec, forming successive fault dislocations with a sliding velocity of probably over 100 cm/sec; at the southern part of the Neodani fault, the rupture produced large fault offsets exceeding 7 m, and then branched off at point c south of Kinbara into the Umehara fault and the deep latent fault; the faulting motion over the entire length was completed within 40 sec. These conclusions, of course, are the results of first approximations, but more detailed treatments would not be significant in view of the quality of the data.

It appears that fault displacements gradually increased during the rupture propagation. Unusually large displacements in the southern part of the Neo-

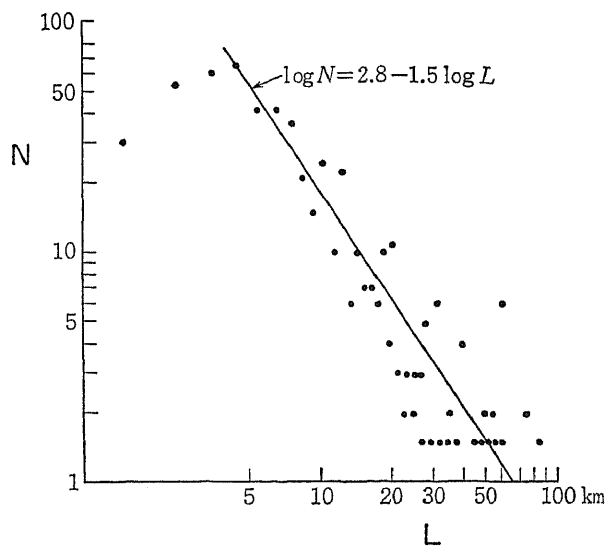

Fig. 14. Number (N) of active geological faults in Japan, plotted against their length in km (L). Data are taken from the results compiled by NCDP (1973).

dani fault may be accounted for by several possible explanations to be described later. The rupture propagation was probably blocked at point c by lateral heterogeneities or possibly by other intersecting geological faults. Large stresses concentrated around there (CHINNERY, 1966) would have caused branching of the rupture into two faults, where fault displacements abruptly decreased due to the divergence of the concentrated energies.

The Nobi earthquake may be regarded as a consequence of the faulting motion of pre-existing Quaternary faults in the Nobi region. Recent seismic observations with high precision have successfully located large and moderate-size, shallow inland earthquakes along pre-existing faults. The distribution of such active faults over Japan is now being extensively investigated by geologists (e.g. MATSUDA *et al.*). In Fig. 14, the number N of active faults are tentatively plotted against their defined length L (NCDP, 1973). The data for lengths longer than 5 km can be fitted to a straight line, with the form $\log N = 2.8 - 1.5 \log L$. It should be noted, however, that this relation cannot be directly correlated with some empirical formulas between the fault length and magnitude or between the magnitude and the annual numbers of earthquakes. This is because the entire length of a pre-existing fault is not always displaced to yield one earthquake, and because the recurrence time for shorter faults would not be the same as for the longer ones.

As can be seen from Fig. 14, the approximate 80 km length of the fault that accompanied the Nobi earthquake was one of the longest, and hence this earthquake was one of the greatest strike-slip type earthquakes that could occur in Japan. The geology in and around the Nobi plain consists of a Paleozoic formation covered by alluvial layers and volcanic ashes. The basement formation extends widely over the western Chubu and eastern Kinki regions, and is bounded on the north by a Tertiary green-tuff area and on the south by the Ryoke metamorphic rock zone. The northern and southern ends of the entire fault of the Nobi earthquake appear to be limited by these geological boundaries. We think that the geological boundaries in basement rocks may be elastic discontinuities that could prevent seismic faulting from further propagation. One reason for the unusually long fault may thus be attributed to the rather uniform geological structure that covers the regions.

7.2 Tectonic stresses

The seismic moment of the Nobi earthquake is estimated as 1.5×10^{27} dyne·cm from the fault dimensions and displacements given in sections 2 and 3, in which we assumed constant fault displacements over the fault depth down to 15 km throughout all segments of the faults. The average stress drop during this earthquake can also be roughly estimated as about 40 bars, which seems rather small compared with that for other Japanese earthquakes (ABE,

1974). However, there could be some difference in the stress drop from place to place, since surface fault displacements vary significantly along the fault direction. For a vertical strike-slip fault in a semi-infinite elastic medium, the stress drop may be approximately given by $\Delta\sigma=\eta\cdot\mu D/W$ (CHINNERY, 1964, 1969), where D, L, W and μ indicate the fault displacement, fault length, fault depth and rigidity, respectively. η is a geometrical factor depending on the aspect ratio W/L of the fault plane, but is almost constant in case of $W/L<1/2$. If we assume that this formula can be approximately applied to the present case except for the branched segments, the stress drop at Kinbara and Kurotsu (between a' and b) is estimated to be about 150 bars and 40 bars respectively. More exact estimates could be made on the basis of a realistic representation for the case of variable dislocations, but the present results should not be very different from these estimates.

The difference in the stress drop between the two sites exceeds 100 bars. Two explanations may be possible for this large difference. One interpretation is that considerably different shear stresses existed before the earthquake depending on the locations, and the corresponding stresses were released. If this is the case, the shear strength of crustal rocks to resist faulting will be different by the same order of magnitude as the stress difference between the two sites. This does not seem unreasonable.

The alternative interpretation is that the initially appiled shear stresses were nearly uniform but the amounts of stress released were appreciably different depending on the locations. The locations which could not resist faulting would release most of the applied stresses, allowing large fault displacements, while the sites which prevented the growth of faulting would release only a fraction of the applied stresses, retaining small fault displacements. If this is the case, the effective factors controlling seismic faulting will be the nature of the fault plane such as the friction, curvature, thickness and strength of pre-existing fault gouges etc. which may vary along the fault line. At this moment, we prefer this interpretation, although there are no measurements to support it. Since the remnant stresses after the earthquake would be almost constant over all segments in the first interpretation, but would be quite different in the alternative one, careful measurements of the in-situ stresses along the fault trace, using modern stress measurement techniques, might be able to give a solution to the problem of which of the interpretations is more realistic.

Figure 15 shows the level changes at several sites near the fault zone over the period of 1884–1940, which have been recompiled here from pre- and post-seismic leveling data (GEOGRAPHICAL SURVEY INST., 1973). Note that these sites have continued to be elevated or subsided during the 25 years after the earthquake up to 1916. The post-seismic movements amount to 9 cm at

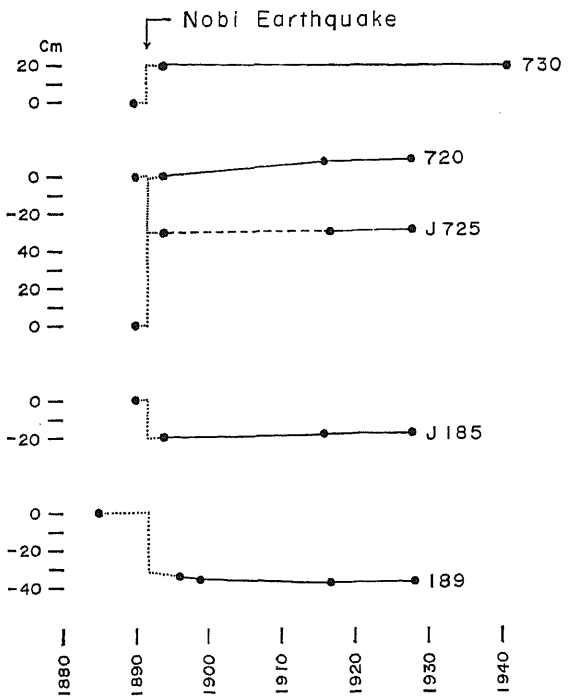

Fig. 15. Secular changes of elevation at several sites near the fault zone, re-arranged from the leveling data by the GEOGRAPHICAL SURVEY INST. (1973).

B.M. 720, 6 cm at B.M. 189, and smaller values at the other sites, which appear proportional to coseismic displacements, though not large enough to discuss in more details. This evidence indicates that the remnant stresses have been gradually released by post-seismic fault movements. The slightly larger displacements at B.M. 189 and 720 a little further from the fault trace than those at J. 185 and 725 suggests that a post-seismic slip might take place in a deeper portion of the crust below the assumed fault depth, as in the case of the San Andreas fault (THATCHER, 1974).

It would be worthwhile to examine possible sources of the stresses that caused the 1891 earthquake. In the western Chubu region, there are several striking Quaternary faults, as seen in Fig. 16, such as the Neodani fault and the Atera fault running in a NNW-SSE direction with a left-lateral slip (SUGIMURA and MATSUDA, 1965), and the Atotsugawa fault with a NE-SW trend with right-lateral offsets (MATSUDA, 1966), making a conjugate set of strike-slip faults. These fracture patterns indicate that the region had been subjected to Quaternary crustal deformation due to compressional tectonic stresses with an E-W trend (SUGIMURA and MATSUDA, 1965; MATSUDA, 1966; HUZITA *et al.*,

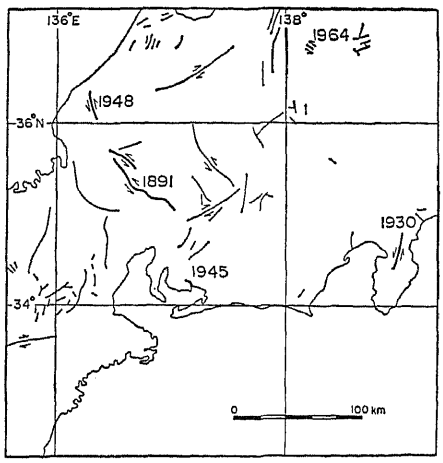

Fig. 16. Distribution of pre-existing Quaternary faults and seismic faults. fine lines; pre-existing faults, thick lines; seismic faults.

1973). Most of the large and moderate shallow earthquakes in this region also indicate left-lateral strike-slip movement along a NW-SE direction (e.g. MIKUMO, 1973b), as in the case of the Nobi earthquake. The maximum compressional stresses for these earthquakes as well as for minor earthquakes (e.g. WATANABE and NAKAMURA, 1967) are oriented nearly in a E-W direction (ICHIKAWA, 1971). It is reasonable to consider that these stresses have been continuously applied to this region since Quaternary ages to the present. One probable source of such compressional stresses may be westward movements and subduction of the Pacific plate below Japan Islands (HUZITA *et al.*, 1973). Another possible source would be the subduction of the Philippine Sea plate along the Nankai trough, and also a spreading of the Japan Sea floor. The former should yield northwestward stresses, and observations of subcrustal earthquakes suggest that the deeper crust in the Outer Zone of southwest Japan is compressed north—northwestward (HUZITA *et al.*, 1973). It does not appear, however, that the above stresses have great effects on the region of interest. The spreading of the Sea of Japan, which had probably originated from the center of the Yamato basin (e.g. KARIG, 1971), would produce southeastward tectonic stresses (TAKEUCHI, 1975). However, the spreading does not seem to continue to the present, since there is no evidence for current active movements since the end of the Tertiary (KARIG, 1971). If this is the case, the Asiatic continental lithosphere gives only resistant stresses against the movement of the Pacific and Philippine Sea plates. More quantitative considerations of these stresses are needed for further investigations.

We are grateful to Professor Ikuei Muramatu of Gifu University, Dr. Tokihiko Matsuda of the Earthquake Research Institute, and Dr. Hiroshi Sato of the Geographical Survey Institute of Japan for providing us various data and their own results with useful comments.

We also wish to thank Drs. Wayne Thatcher of the U.S. Geological Survey, Menlo Park and George Zandt of MIT for their critical reading of the manuscript. Our thanks are extended to Mrs. Ritsuko Koizumi and Mr. Yoshinobu Hoso for assistance in the present work.

Computations were made at the Data Processing Center of Kyoto University.

REFERENCES

ABE, K., Seismic displacements and ground motion near a fault: The Saitama earthquake of September 21, 1931, *J. Geophys. Res.*, **79**, 4393–4399, 1974.

AOKI, H., T. TADA, Y. SASAKI, T. OOIDA, I. MURAMATU, H. SHIMAMURA, and I. FURUYA, Crustal structure in the profile across central Japan as derived from explosion seismic observations, *J. Phys. Earth*, **20**, 197–223, 1972.

BESSHO, B., Unusual tectonic movements, *Rep. Geol., Kanazawa Univ.*, **1**, 1–364, 1967 (in Japanese).

CHINNERY, M. A., The strength of the earth's crust under horizontal shear stress, *J. Geophys. Res.*, **69**, 2085–2089, 1964.

CHINNERY, M. A., Secondary faulting I: Theoretical aspects, *Can. J. Earth Sci.*, **3**, 163–174, 1966.

CHINNERY, M. A., Theoretical fault models, *Publ. Dom. Obs., Ottawa*, **37**, 211–223, 1969.

GEOGRAPHICAL SURVEY INSTITUTE, Vertical movements in Chubu district (I), *Rep. Coord. Comm. for Earthquake Prediction*, **9**, 74–78, 1973 (in Japanese).

GIFU OBSERVATORY, *Report on the Great Nobi Earthquake of 1891*, 1894 (in Japanese).

HASKELL, N. A., Elastic displacements in the near-field of a propagating fault, *Bull. Seismol. Soc. Am.*, **59**, 865–908, 1969.

HUZITA, K., Y. KISHIMOTO, and K. SHIONO, Neotectonics and seismicity in the Kinki area, *Geosciences, Osaka City Univ.*, **16**, 93–124, 1973.

ICHIKAWA, M., Reanalyses of mechanism of earthquakes which occurred in and near Japan, and statistical studies on the nodal plane solutions obtained, 1926–1968, *Geophys. Mag.*, **35**, 207–274, 1971.

IIDA, K. and H. AOKI, Gravity anomalies and subterranean mass distribution, with special reference to the Nobi plain, Japan, *J. Geod. Soc., Japan*, **5**, 88–91, 1959 (in Japanese).

JAPAN METEOROLOGICAL AGENCY, *Q.J. Seismology*, **22**, *Suppl. Vol.*, 1957.

KARIG, D. E., Origin and development of marginal basins in the western Pacific, *J. Geophys. Res.*, **76**, 2542–2561, 1971.

KOTO, B., On the cause of the great earthquake in central Japan, *J. Coll. Sci., Imp. Univ. Tokyo*, **5**, 295–353, 1893.

MANSINHA, L. and D. E. SMYLIE, The displacement fields of inclined faults, *Bull. Seism. Soc. Am.*, **61**, 1433–1440, 1971.

MARUYAMA, T., On the force equivalents of dynamical elastic dislocations with reference to the earthquake mechanism, *Bull. Earthq. Res. Inst.*, **41**, 467–486, 1963.

MARUYAMA, T., Static elastic dislocations in an infinite and semi-infinite medium, *Bull. Earthq. Res. Inst.*, **42**, 289–368, 1964.

MATSUDA, T., Strike-slip faulting along the Atotsugawa fault, *Bull. Earthq. Res. Inst.*, **44**, 1179–1212, 1966 (in Japanese).

MATSUDA, T., Surface faults associated with Nobi (Mino-Owari) earthquake of 1891, Japan, *Spec. Rep. Earthq. Res. Inst.*, **13**, 85–126, 1974 (in Japanese).

MIKI, H., H. WATANABE, and M. SHIMADA, Observations of ultra-microearthquakes in the vicinity of Neo Valley fault in central Honshu, Japan, *Zisin*, **18**, 103–112, 1965 (in Japanese).

MIKUMO, T., Faulting process of the San Fernando earthquake of February, 9, 1971, inferred

from static and dynamic near-field displacements, *Bull. Seism. Soc. Am.*, **63**, 249–269, 1973a.

MIKUMO, T., Faulting mechanism of the Gifu earthquake of September 9, 1969, and some related problems, *J. Phys. Earth*, **21**, 191–212, 1973b.

MURAMATU, I., Magnitude of the Nobi earthquake of Oct. 28, 1891, *Zisin*, **15**, 341–342, 1962 (in Japanese).

MURAMATU, I., Distribution of seismic intensity and crustal deformation in the region destroyed by the great Nobi earthquake of October 28, 1891, *Res. Rep., Gifu Univ.*, **3**, 202–224, 1963 (in Japanese).

MURAMATU, I., Y. ENDO, H. SIMONO, H. KOOKETU, and S. SUZUKI, Observation of microearthquakes in Mino district in Gifu Prefecture, central Japan, *J. Phys. Earth*, **11**, 35–48, 1963.

MUTO, K. and Y. KAWABATA, Vertical displacements of bench marks in the Nobi and other districts, *Bull. Earthq. Res. Inst.*, **11**, 315–323, 1933 (in Japanese).

NATIONAL CENTER FOR DISASTER PREVENTION (NCDP), *Explanatory text of the Quaternary tectonic map of Japan*, 1973.

OMORI, F., *General Report on the Nobi Earthquake, Gifu Observatory*, pp. 48–88, 1894 (in Japanese).

OMORI, F., Note on the Great Mino-Owari Earthquake of Oct. 28th, 1891, *Publ. Earthq. Inv. Comm.*, **4**, 13–24, 1900.

OMORI, F., On classification of earthquakes, *Publ. Earthq. Inv. Comm., A*, **68**, 3–19, 1910 (in Japanese).

OOIDA, T., I. YAMADA, T. TADA, K. ITO, K. SUGIYAMA, and Y. SASAKI, Microearthquake activity in central Honshu, Japan, Part 1. Seismicity of microearthquakes in the vicinity of the Neo Valley fault, *Zisin*, **24**, 240–247, 1971 (in Japanese).

SASAKI, Y., S. ASANO, I. MURAMATU, M. HASHIZUME, and T. ASADA, Crustal structure in the western part of Japan derived from the observation of the first and second Kurayoshi and the Hanabusa explosions, *Bull. Earthq. Res. Inst.*, **48**, 1129–1136, 1970.

SATO, H., A study of horizontal movement of the earth crust associated with destructive earthquakes in Japan, *Bull. Geogr. Survey Inst.*, **19**, 89–130, 1974.

SUGIMURA, A. and T. MATSUDA, Atera fault and its displacement vectors, *Geol. Soc. Am. Bull.*, **76**, 509–522, 1965.

SUGISAKI, R. and K. SHIBATA, Geochemical study on ground water (I)—Surface geology and aquifers in the Nobi plain, *J. Geol.*, **67**, 335–345, 1961 (in Japanese).

TAKEUCHI, H., Plate Tectonics, Spec. Ed., *Scientific American*, (Japanese edition), pp. 84–95, 1975.

THATCHER, W., Strain release mechanism of the 1906 San Francisco earthquake, *Science*, **184**, 1283–1285, 1974.

USAMI, T., Descriptive table of major earthquakes in and near Japan which were accompanied by damages, *Bull. Earthq. Res. Inst.*, **44**, 1571–1622, 1966 (in Japanese).

UTSU, T., Aftershocks and earthquake statistics (I)—Some parameters which characterize an aftershock sequence and their interpretations, *J. Fac. Sci., Hokkaido Univ., Ser. VII*, **3**, 129–195, 1969.

WATANABE, H. and M. NAKAMURA, Some properties of microearthquakes in the vicinity of the Neo Valley fault, central Honshu, Japan, *Zisin*, **20**, 106–115, 1967 (in Japanese).

YOKOO, Y. and T. HORIUCHI, *Map of Ground Structures in Nagoya*, Corona Publ. Co., 1969.